C.P. No. 104
(14,449)
A.R.C. Technical Report

MINISTRY OF SUPPLY

AERONAUTICAL RESEARCH COUNCIL

CURRENT PAPERS

# The Effect of Endplates on Swept Wings

By

D. Kuchemann and D. J. Kettle

LONDON: HER MAJESTY'S STATIONERY OFFICE

1952

Price 4s. 0d. net

C.P.104

Report No. Aero.2429

June, 1951

ROYAL AIRCRAFT ESTABLISHMENT

# The effect of endplates on swept wings

by

D. Küchemann
and
D. J. Kettle

---

## SUMMARY

Existing methods of calculating the effect of endplates on straight wings are modified so as to apply to swept wings. The changes in overall lift and drag, and also the spanwise distribution of the additional load, can be calculated.

The theoretical results are compared with experimental results obtained on swept wings, including new measurements of lift, drag and pitching moment, made on an untapered 45° sweptback wing of aspect ratio 3 at low speed.

The method of calculation is also extended to cover the effect of the tip vortex which is formed on wings without endplates.

---

## LIST OF CONTENTS



## LIST OF ILLUSTRATIONS

## 1 Introduction

The theory developed for an unswept wing with endplates has proved useful in estimating the effect of fins at or near a wing tip, and the interaction of tailplane and fin. The present note gives a method of modifying the calculation to apply to swept wings without camber and twist. A comparatively simple change is made, based on the method developed in Ref.3. Overall lift and drag due to endplates can be determined, and also the change in span loading. The pitching moment on swept wings is also affected.

To check the method of calculation, measurements of lift, drag and pitching moment were made on an untapered 45° sweptback wing of aspect ratio 3 with and without endplates. It will be seen that the $C_L$ range in which the endplates are effective is subject to scale effect, and further tests at full scale Reynold's numbers are desirable.

The method of calculation is also extended to cover the effect of the tip vortex, which is formed on wings without solid endplates. Within a certain incidence range a sheet of trailing vortices is produced which is similar to that produced by a wing with solid endplates. On swept wings there is an appreciable change of pitching moment due to this vortex, and this can be predicted with a fair degree of accuracy.

## 2 The effects of solid endplates

### 2.1 Application of the theory developed for straight wings to the overall lift and drag of swept wings

The existing theory for endplates on straight wings[1,2] deals only with such arrangements as give minimum induced drag at a prescribed total lift. For these arrangements the spanwise load distribution is such that the induced downwash (the induced velocity component, in the opposite sense to the lift) is constant along the wing span. Since the wake follows the direction of the undisturbed flow, if we apply the linearized lifting line theory, the load distribution is determined by the spanwise section of the wing plus endplates (which is equal to the section of the wake) and the magnitude of the downwash Then the planform $c(y)$ of a wing with symmetrical section is determined by the load distribution. The resulting effect of the endplates is to increase the effective aspect ratio A by a factor $\frac{1}{\kappa}$, which mainly depends on the height of the endplates in relation to the wing span (see Fig.1).

When generalizing this concept for a swept wing with endplates, we may still assume (Ref.3, Section 6.1) that the induced incidence $\alpha_i$ is constant along the chord and is equal to half the value of the induced incidence at a great distance behind the wing. Thus the shape of the wake and the load distribution are the same in both cases, for a straight and for a swept wing. The values $\kappa$ obtained for straight wings with endplates can also be used for swept wings with endplates (in the optimum case of minimum induced drag).

The overall lift slope of a swept wing, however, is different from that of an unswept wing. For wings with minimum induced drag*,

---

* As shown in Section 6.1 of Ref.3, the planform is not elliptic for a sweptback wing with minimum induced drag. It is, in fact, more highly tapered.

$$\frac{\bar{C}_{L_W}}{\alpha} = \frac{a_o \cos\varphi}{1 + \frac{a_o \cos\varphi}{\pi A}} = \frac{2\pi \cos\varphi}{1 + \frac{2 \cos\varphi}{A}} \quad \text{for } a_o = 2\pi, \qquad (1)$$

where $a_o$ is the lift slope of the two-dimensional aerofoil section, $\varphi$ the angle of sweep of the $\frac{c}{4}$ - line, and $A$ the aspect ratio of the wing. This relation follows from equations (31) and (32) in Ref.3. Thus for a swept wing we obtain the same relation as exists for an unswept wing if we replace the sectional lift slope $a_o$ by $a_o \cos\varphi$, the lift slope of a sheared wing of infinite span (see equation (11) in Ref.3). The effective aspect ratio of the wing with endplate being $\frac{A}{\kappa}$, we obtain for its overall lift coefficient

$$\frac{\bar{C}_L}{\alpha} = \frac{a_o \cos\varphi}{1 + \kappa \frac{a_o \cos\varphi}{\pi A}} = \frac{2\pi \cos\varphi}{1 + \kappa \frac{2 \cos\varphi}{A}} \quad \text{for } a_o = 2\pi \qquad (2)$$

Hence, at the same incidence $\alpha$,

$$\frac{\bar{C}_L}{\bar{C}_{L_W}} = \frac{1 + \frac{a_o \cos\varphi}{\pi A}}{1 + \kappa \frac{a_o \cos\varphi}{\pi A}}, \qquad (3a)$$

or

$$\frac{\Delta \bar{C}_L}{\bar{C}_{L_W}} = \frac{\bar{C}_L - \bar{C}_{L_W}}{\bar{C}_{L_W}} = \frac{a_o \cos\varphi}{\pi A} \frac{1 - \kappa}{1 + \kappa \frac{a_o \cos\varphi}{\pi A}} \qquad (3b)$$

It is proposed to use this difference formula to compute the endplate effect for a wing of any span loading whose lift coefficient is $\bar{C}_{L_W}$.

The minimum induced drag of a wing without endplates, whether it is swept or not, is given by:-

$$\bar{C}_{D_{i_W}} = \frac{\bar{C}_{L_W}^2}{\pi A} \qquad (4)$$

(see Ref.3, section 6.1). Thus, for the wing with endplates,

$$\bar{C}_{D_i} = \kappa \frac{\bar{C}_L^2}{\pi A} \qquad (5)$$

The drag difference, at the same value of $\bar{C}_L$, is then:-

$$\Delta \bar{C}_{D\,i} = \bar{C}_{D\,i} - \bar{C}_{D\,i_W} = -(1-\kappa)\frac{\bar{C}_L^{\,2}}{\pi A}.$$

This shows that the reduction of the drag due to endplates does not depend on the angle of sweep, whereas the increase of lift is smaller for swept wings than for straight ones.

Values for $\kappa$ can be found in Refs.1 and 2 for various endplate arrangements including wings with and without dihedral and wings with one endplate only. The values for $\kappa$ for common arrangements are replotted in Fig.1. $\kappa$ depends only on the geometry of the wing-endplate arrangement: When the wing stops at the endplate, it depends only on the ratio between height of endplate and span of wing.

2.2 The spanwise loading of a swept wing with endplates

The reduction of the drag and the increase in total lift are connected with a modification of the spanwise loading of the wing. Most of the lift increment is produced near the endplate and, with swept wings, this lift increase will contribute appreciably to the pitching moment of the wing. Further, this lift increase near the tips might intensify the tendency to tip stalling. It is, therefore, of interest to know in a practical case the spanwise loading of the swept wing with endplates.

The method in Refs.1 and 2 does not give the spanwise loadings of a given wing both with and without endplates, but only those of an elliptic wing without endplates and of another wing with endplates, each giving minimum induced drag. It is assumed here that the difference in spanwise loading between the two minimum induced drag wings can be taken as the difference in spanwise loading due to endplates for a given wing; and further, that this is justified even though the spanwise loading of the wing without endplates may not be elliptic but that of a swept wing. With these assumptions the difference in spanwise loading can be taken from the results in Refs.1 and 2 and then added to the basic spanwise loading of the wing alone, which can be worked out by the method of Ref.3.

Let the spanwise loading of the minimum induced drag wing with endplates be

$$\frac{C_L(\eta)\, c(\eta)}{\bar{C}_L \cdot \bar{c}} = \ell\left(\eta; \frac{h}{b}\right),$$

where $C_L(\eta)$ is the local lift coefficient, $c(\eta)$ and $\bar{c}$ local and mean chords respectively, and $\eta = \frac{2y}{b}$ the spanwise coordinate (normal to free stream).

With

$$\frac{C_{L_W}(\eta)\, c(\eta)}{\bar{C}_{L_W}\, \bar{c}} = \ell_W(\eta) = \frac{4}{\pi}\sqrt{1-\eta^2}$$

as the spanwise loading of the minimum induced drag wing without endplates $(h = 0)$ the difference due to endplates is

$$\Delta c_L(\eta)\,\frac{c}{\bar{c}}(\eta) = [c_L(\eta) - c_{L_W}(\eta)]\,\frac{c}{\bar{c}} = \bar{c}_{L_W}\left[\frac{\bar{c}_L}{\bar{c}_{L_W}}\,\ell\left(\eta;\frac{h}{b}\right) - \ell_W(\eta)\right]$$

Substituting for $\frac{\bar{c}_L}{\bar{c}_{L_W}}$ from equation (3a), we obtain

$$\Delta c_L(\eta)\,\frac{c}{\bar{c}}(\eta) = \bar{c}_{L_W}\left\{\frac{1+\frac{a_o\cos\varphi}{\pi A}}{1+\kappa\frac{a_o\cos\varphi}{\pi A}}\,\ell\left(\eta,\frac{h}{b}\right) - \ell_W(\eta)\right\} \qquad (7)$$

In this relation $\bar{c}_{L_W}$ may be replaced by the corresponding value for an actual wing, and $\Delta c_L$ may be added to their $c_{L_W}$ - distribution of the actual wing without endplates.

The functions $\ell\left(\eta,\frac{h}{b}\right)$ and $\ell_W(\eta)$ do not depend on the angle of sweep, and they can be taken from the results in Refs.1 and 2 for straight wings. Curves of $\ell\left(\eta,\frac{h}{b}\right)$ for the simple case of symmetrical endplates at the wing tips are plotted in Fig.2*. They can also be used for the cases where the endplates are asymmetrically placed at the tip, including the extreme cases where they are either entirely above or below the wing. The differences in spanwise loadings between these extreme cases are very small.

This method has been applied to a 40° sweptback wing with circular endplates, of diameter equal to the tip chord, and the results are compared with experimental results from Ref.4 in Fig.3. The agreement is good at small incidences for the spanwise loadings of both the wing alone and the wing with endplates. With increasing incidence, however, there is the well known reduction of lift due to the thickened boundary layer and, more pronounced still, a breakdown of the flow near the tips. This is caused by the high suction peaks near the leading edge in that region. This effect will be discussed in more detail in section 2.32.

## 2.3 Low speed tunnel tests on a 45° sweptback wing with endplates

### 2.31 Description of model and tests

A sketch of the model is given in Fig.4. The aspect ratio of the wing was 3 and the wing section R.A.E.103 having a thickness-chord ratio of 0.12. The wing had a constant chord with the tips cut parallel to the centre line. The shape of the endplate, in side view, was similar to that of a tip tank of fineness ratio 8 : 1, and height = 0.3c = 0.1b.

---

* Curves given in Refs.1 and 2 are for a function $\frac{\Gamma}{\omega\,\frac{b}{2}}$, which is related to $\ell\left(\eta,\frac{h}{b}\right)$ by $\ell\left(\eta,\frac{h}{b}\right) = \frac{2\kappa}{\pi}\cdot\frac{\Gamma}{\omega\,\frac{b}{2}}$.

Measurements of lift, drag and pitching moment were made on the plain wing and with endplates in three positions (upper, central and lower) as shown in Fig.4. These tests were made at windspeeds of 100, 120 and 180 ft/sec, corresponding to Reynolds' numbers of 0.63, 0.75 and $1.13 \times 10^6$ respectively. In addition, pressures were measured using "creepers", on the centre line chord of the plain wing and in the junction of wing and central endplate at a windspeed of 120 ft/sec.

The tests were made in the 5ft open jet wind tunnel of the R.A.E. during June 1950.

2.32 Results

The overall values obtained for lift, drag and pitching moment are plotted in Figs.5-7. The wing without endplates shows a very marked reduction of lift due to boundary layer up to incidences of about 12°, and a subsequent lift increase from the tip vortex effect (see section 3). The wing with endplates has a higher lift slope at low incidences; the lift reduction from boundary layer appears to be smaller; and the effect of the tip vortex is less noticeable. The values of $\bar{C}_{L_{max}}$ are lower than those obtained on the wing alone, and are summarised below. There is a scale effect, similar to that occurring on the wing alone.

| Case \ Reynolds' Number | | $0.63 \times 10^6$ | $0.75 \times 10^6$ |
|---|---|---|---|
| $\bar{C}_{L_{max}}$ | wing alone | 0.95 | 0.99 |
| $\bar{C}_{L_{max}}$ | wing with endplates in central position | 0.87 | 0.91 |

The values of $\bar{C}_{L_{max}}$ with the endplates in the upper and central positions are less than that for the lower position.

The drag curves of the wing alone show a very marked deviation from the drag as estimated for non-viscous flow. This is due to the low Reynolds' number of the test; the effect has been described in more detail in Ref.5. This deviation remains with the endplates in position. At low values of $C_L$ (below about 0.5) the value of the induced drag factor K for the wing alone varies slightly with Reynolds' number. K = 1.38 at R.N. = $0.75 \times 10^6$, compared with a theoretical value of 1.09 for non-viscous flow.

The pitching moment curves (referred to the mean $\frac{c}{4}$ line) are also affected by Reynolds' number, both with and without endplates. The stable region above $C_L = 0.6$, which is caused by the tip vortex, is less pronounced with endplates in position. At the same time, a breakdown of the flow on the upper surface of the wing endplate junction reduces the stability.

In Figs.8 and 9 the measured changes of lift and drag are compared with the calculated values. The effects are small because of the small

height of the endplates in relation to the span of the wing, $\left(\frac{h}{b} = 0.1\right)$ and this affects the accuracy of the differences obtained. However, the changes appear as predicted by calculation up to a $C_L$ of about 0.5. Above this value, the drag rises suddenly, as on the wing alone. The $C_L$ value at which the drag curve begins to deviate from the calculated curve increases with Reynolds' number. At this point, the increase in lift also falls off. The lower endplate position is beneficial in this respect, probably because there is only one junction with the wing, instead of two in the symmetrical case. This is confirmed by N.A.C.A. results[8] obtained on an untapered 45° sweptback wing of aspect ratio 2.0. Some of the results have been extracted and are shown in Fig.10. In the case of an endplate extending above and below the wing surface, the deviation of the drag curve from the calculated curve occurs at a lower value of $C_L$ than in the case of an endplate extending only on the lower surface.

It is not known how far this deviation from non-viscous flow would be delayed by increasing the Reynolds' number up to full scale. On straight wings, tests (see for example Ref.1) have shown that the beneficial effect of endplates extends through the whole $C_L$ range, and even $C_{L_{max}}$ is slightly higher with endplates. This cannot be expected, however, for endplates on sweptback wings. Here the endplate produces at the wing tip the same type of chordwise lift distribution as is found at the centre of a sweptforward wing, which has a very pronounced suction peak near the leading edge, and brings about a premature stall. This is shown in Fig.11, where the measured pressure distributions in the endplate junction are plotted and compared with those at the centre line of the wing.

Obviously, the high peak in the junction has led to a local separation of the flow, apparent at $\alpha = 8.2°$, which corresponds to $C_L = 0.4$. A similar breakdown occurred in the case shown in Fig.3, between $\alpha = 5°$ and 10°. Modifications to the wing shape in the tip region, such as camber and twist, would be necessary to remedy this.

## 3 Application of endplate theory to the tip vortex

For straight wings, the methods used here have already been applied by W. Mangler in 1939[6] to estimate the effect of the tip vortex at small aspect ratios. A slightly different approach is used in the present instance.

Tuft observations on an untapered 45° sweptback wing of A.R.3[5] showed that the equalising flow round the edge of the wing tip (from the lower surface towards the upper surface of the wing) separates from the surface at a certain incidence $\alpha_s$. The value of $\alpha_s$ will depend on the Reynolds' number and on the tip shape. From this separation, a vertical vortex sheet is formed which joins the ordinary sheet of trailing vortices at the trailing edge of the wing tip. A cross section through the vortex sheet in a vertical plane behind the wing has the same shape as that obtained in the same position behind a solid endplate of the same height. Such distributions of vorticity have already been observed by A. Fage and L.F.G. Simmons in 1925[7].

The separation begins at the trailing edge of the tip section and gradually extends forward over the whole tip chord $C_T$ as the incidence increases. This stage is completed when the flow begins to break down at the leading edge of the outer part of the wing. The angle of incidence

at which this occurs is called $\alpha_m$. The value of $\alpha_m$ depends also on the Reynolds' number. For simplicity, it is assumed here that the separation point moves forward linearly with incidence, between $\alpha_s$ and $\alpha_m$. Assuming that the upper edge of the vertical vortex sheet lies along the direction of the free stream, we obtain for the height h of this "endplate vortex", see Fig.12:-

$$\frac{h}{b} = \alpha \frac{\alpha - \alpha_s}{\alpha_m - \alpha_s} \cdot \frac{C_T}{b} \qquad (8)$$

Thus, the height becomes smaller with increasing taper of the wing. Also, the value of $\frac{h}{b}$ and thus the tip vortex effect becomes smaller with increasing aspect ratio. Knowing $\frac{h}{b}$, the changes of lift and drag can be calculated as described in sections 2.1 and 2.2.

Experimental pressure distributions given in Ref.5 show that the additional load due to the tip vortex is mostly concentrated at the rear of the section. For estimation purposes it may be sufficient to assume the load to be concentrated on the $\frac{3c}{4}$ line. In addition this means that an induced drag increment is produced by the interaction of the bound vortices. The system of trailing vortices, however, may still be assumed to be the same as that which gives minimum induced drag.

On swept wings, the main effect of this endplate vortex is to give a nose-down moment about the mean $\frac{c}{4}$ point. It can be obtained from the spanwise distribution of the additional load, assuming that this acts on the $\frac{3c}{4}$ line. Estimated pitching moments using this method are compared in Fig.12 with experimental results obtained on an untapered 45° sweptback wing of aspect ratio 3 from Ref.5. In this case, $\alpha_m$ was known to be between 19° and 20°. The value of $\alpha_s$ was taken to be 5° and 10°, which roughly corresponds to the incidences of separation at the lowest and highest Reynolds' numbers of the test. Considering the large number of assumptions made, and the unknown effect of the thickened boundary layer on the wing, the agreement between measured and calculated curves is good.

## 4 Conclusions

It has been shown how existing methods of calculating the effect of endplates on straight wings can be modified to determine the changes in overall lift and drag as well as the spanwise distribution of the additional load on swept wings. Comparisons with experimental results show that the effect of the endplates is as predicted in the low $C_L$ range (up to a $C_L$ of about 0.5 at the low Reynolds' number of the test) at $C_L$ values above 0.5, high suction peaks in the "sweptforward" endplate junction lead to a breakdown of the flow and cause a loss of endplate effectiveness. This effect is delayed to higher values of $C_L$ with endplates which extend only on the lower surface of the wing. The $C_L$ range over which the endplates are effective at full scale Reynolds' numbers, and the influence of compressibility still remain to be investigated.

The method is also used to estimate the change of pitching moment caused by the tip vortex which is formed on wings without endplates. Reasonable agreement between estimated and measured pitching moments is obtained.

## REFERENCES


| No. | Author | Title, etc. |
|---|---|---|
| 1 | F. Nagel | Flügel mit seitlichen Scheiben<br>Mitt d. AVA 1924<br>Ergeb.d. AVA III Lieferung, p.17 and p.95 |
| 2 | W. Mangler and<br>J. Rotta | Aerofoils with tip plates. M.S.O. - AVA<br>Monograph F, 1.6, R & T 1023, 1947 |
| 3 | D. Küchemann | A simple method for calculating the span and chordwise loadings on thin swept wings<br>ARC 13,758, August, 1950 |
| 4 | Ingelmann and<br>Sundberg | Experimental determination of pressure distributions on a plane wing with 40° sweepback at low speed<br>Swedish Report KTH - Aero T.N.8, 1949 |
| 5 | J. Weber and<br>G. G. Brebner | Low speed tests on a 45° sweptback wing<br>ARC 13,655, May, 1950 |
| 6 | W. Mangler | Der kleinste induzierte Widerstand eines Tragflügels mit kleinem Seitenverhältuis<br>Jahrb 1939 d. Deutschen Luftfahrtforschung<br>P.I, 139 |
| 7 | A. Fage and<br>L. F. G. Simmons | An investigation of the airflow pattern in the wake of an aerofoil of finite span<br>R & M 951, 1925 |
| 8 | J. M. Riebe and<br>J. M. Watson | The effect of endplates on swept wings at low speed<br>N.A.C.A. Tech. Note 2229, 1950 |


---

## LIST OF SYMBOLS

$c$ = wing chord

$b$ = wing span

$A$ = aspect ratio

$h$ = height of endplate

$\alpha$ = geometric angle of incidence

$\varphi$ = angle of sweep of $\frac{c}{4}$ line

$V_o$ = velocity of main flow

## LIST OF SYMBOLS (Contd)

$C_p$ = pressure coefficient

$C_L$ = local lift coefficient of section

$\overline{C}_{L_W}$ = total lift coefficient of wing alone

$\overline{C}_L$ = " " " " " with endplate

$a_o$ = lift slope coefficient of the two dimensional aerofoil (usually taken as $2\pi$)

$\overline{C}_{D_W}$ = total drag coefficient of wing alone

$\overline{C}_D$ = " " " " " with endplate

$\overline{C}_{D_i}$ = total induced drag coefficient

$C_m$ = pitching moment coefficient of section

$\overline{C}_m$ = total pitching moment coefficient

---



*Wt.2078.CP.104.K3. Printed in Great Britain.*

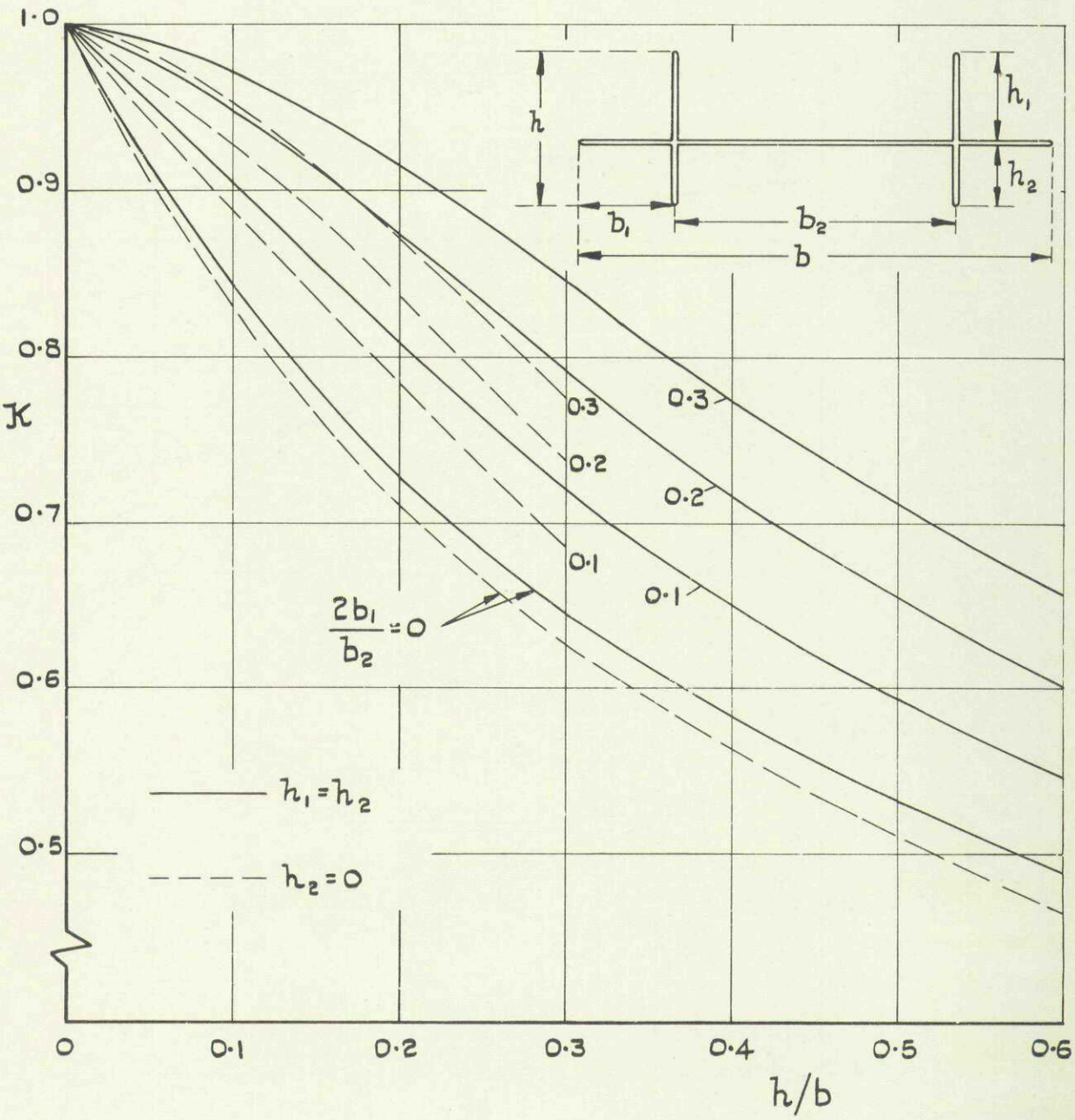


FIG.1. VARIATION OF FACTOR K WITH ENDPLATE HEIGHT AND WING SPAN.

FIG.2.

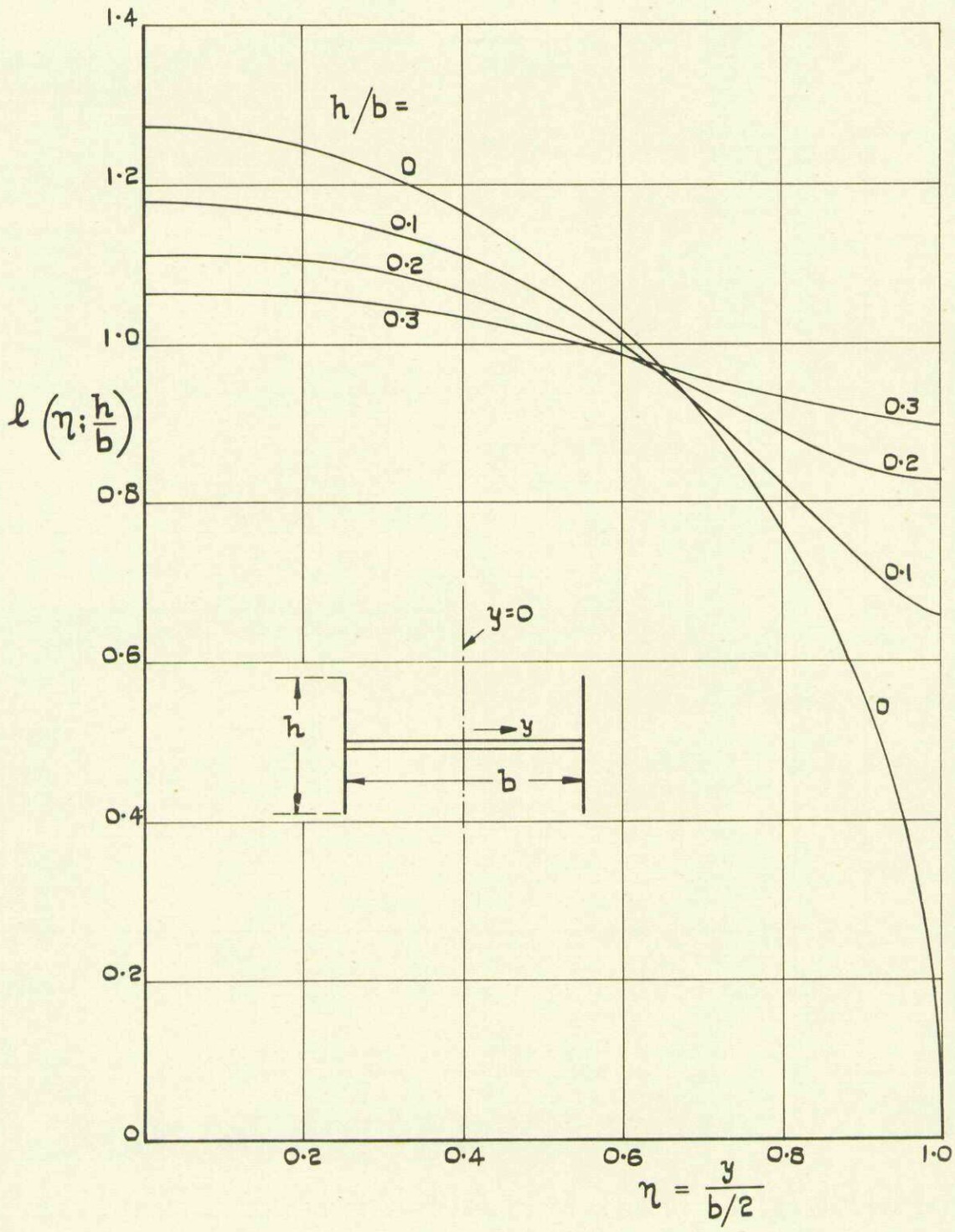


FIG.2. VARIATION OF FUNCTION $\ell\left(\eta;\frac{h}{b}\right)$.

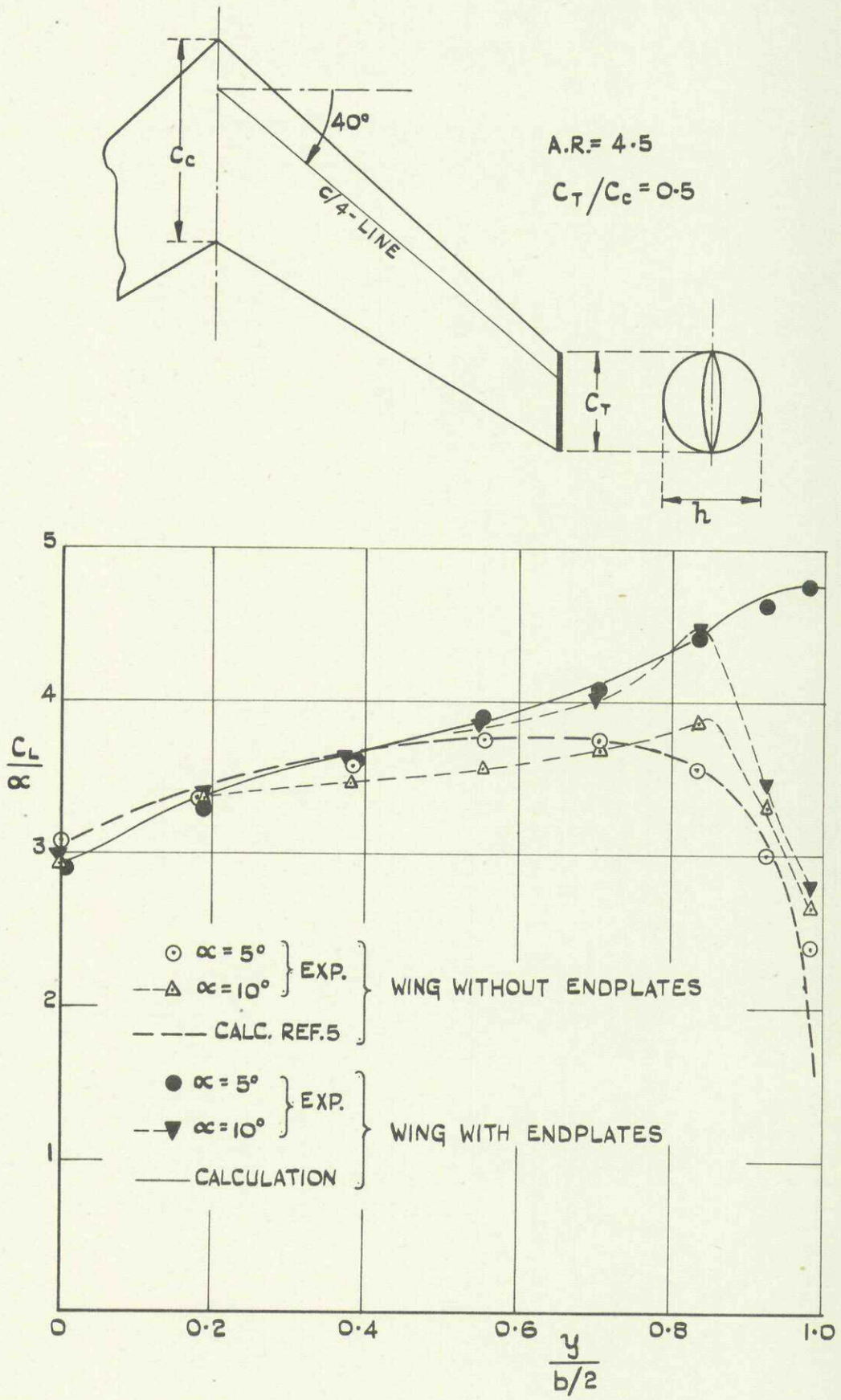


FIG.3. SPANWISE DISTRIBUTION OF LOAD WITH & WITHOUT ENDPLATES. COMPARISON OF THEORY WITH EXPERIMENT (REF. 4.)

FIG .4.

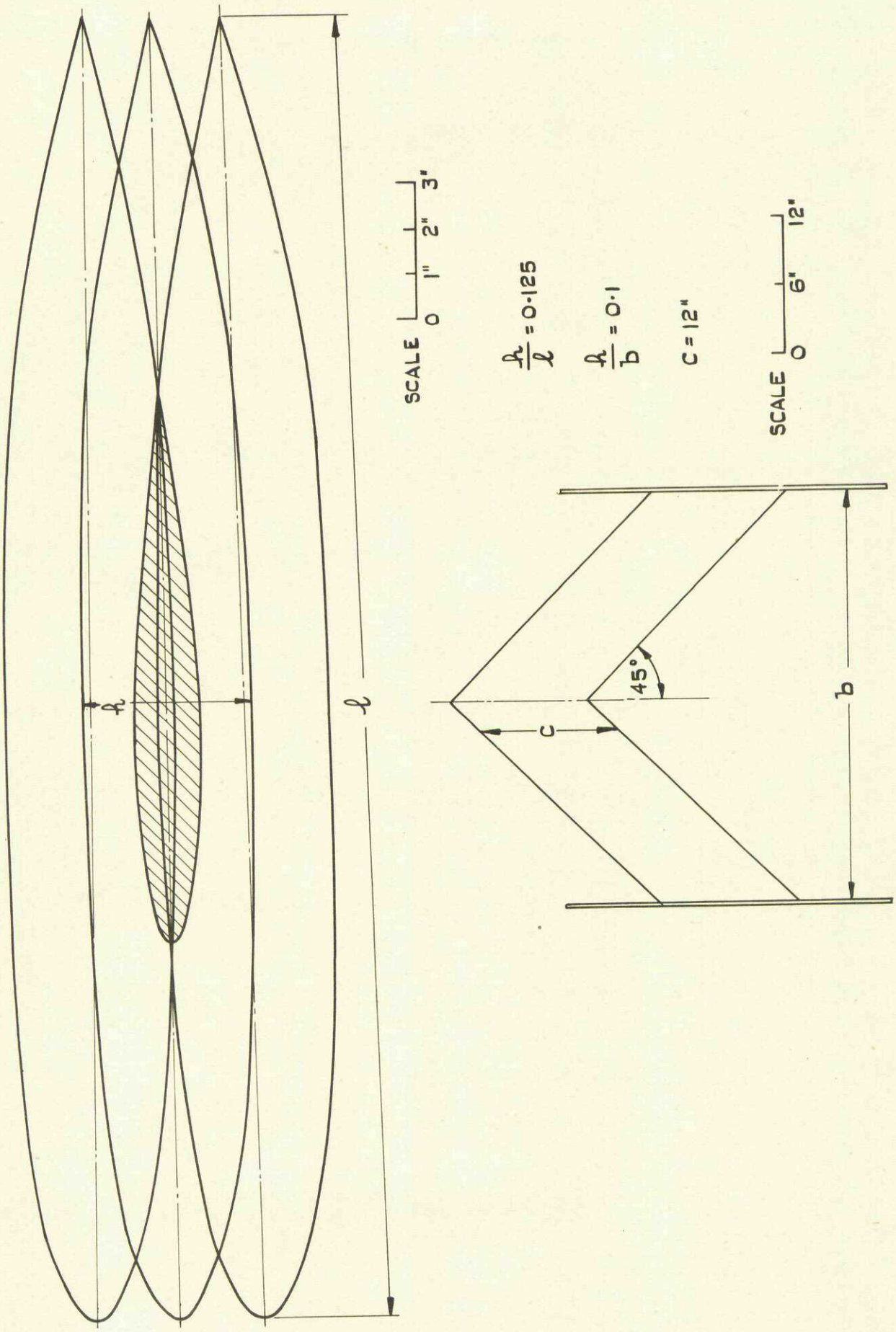


FIG. 4. SKETCH OF 45° SWEPTBACK WING WITH ENDPLATES IN THREE POSITIONS.

FIG .5.

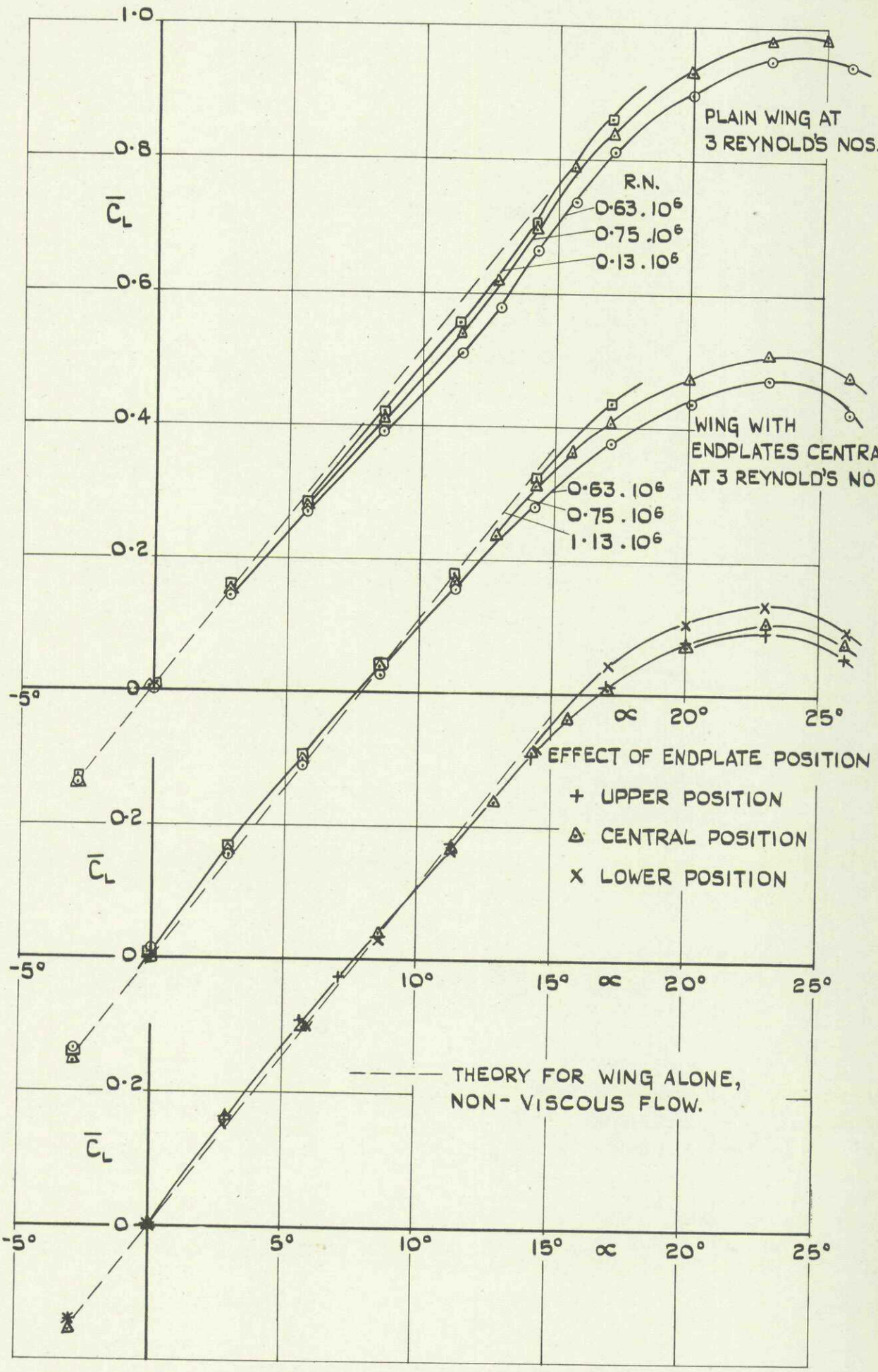


FIG.5. LIFT COEFFICIENT vs $\alpha$.
EFFECT OF ENDPLATES ON 45° SWEPTBACK WING.
(A.R. = 3·0.)

FIG.6.

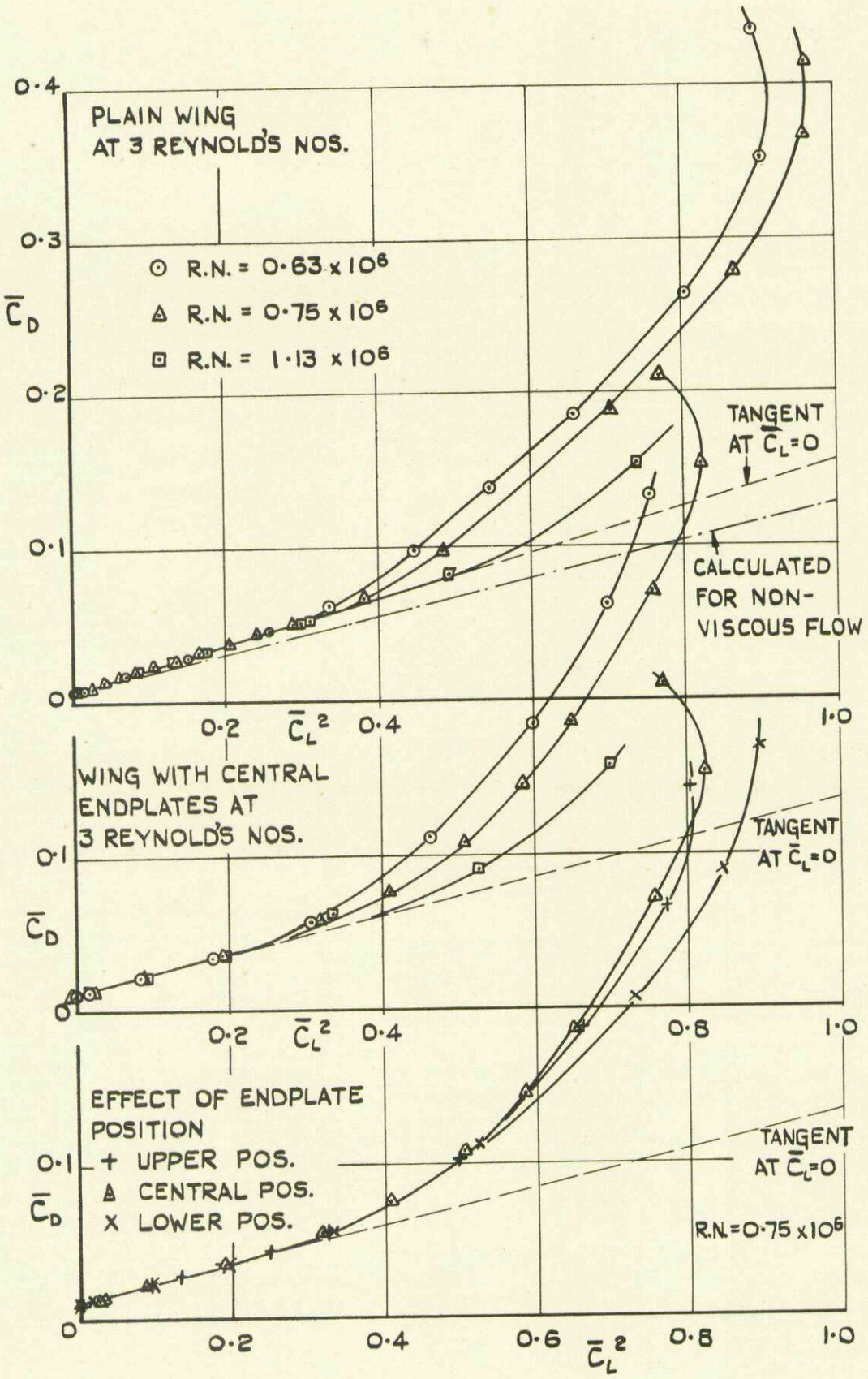


FIG.6. DRAG COEFFICIENT vs $C_L^2$
EFFECT OF ENDPLATES ON 45° SWEPTBACK WING
(A.R.= 3·0)

FIG. 7.

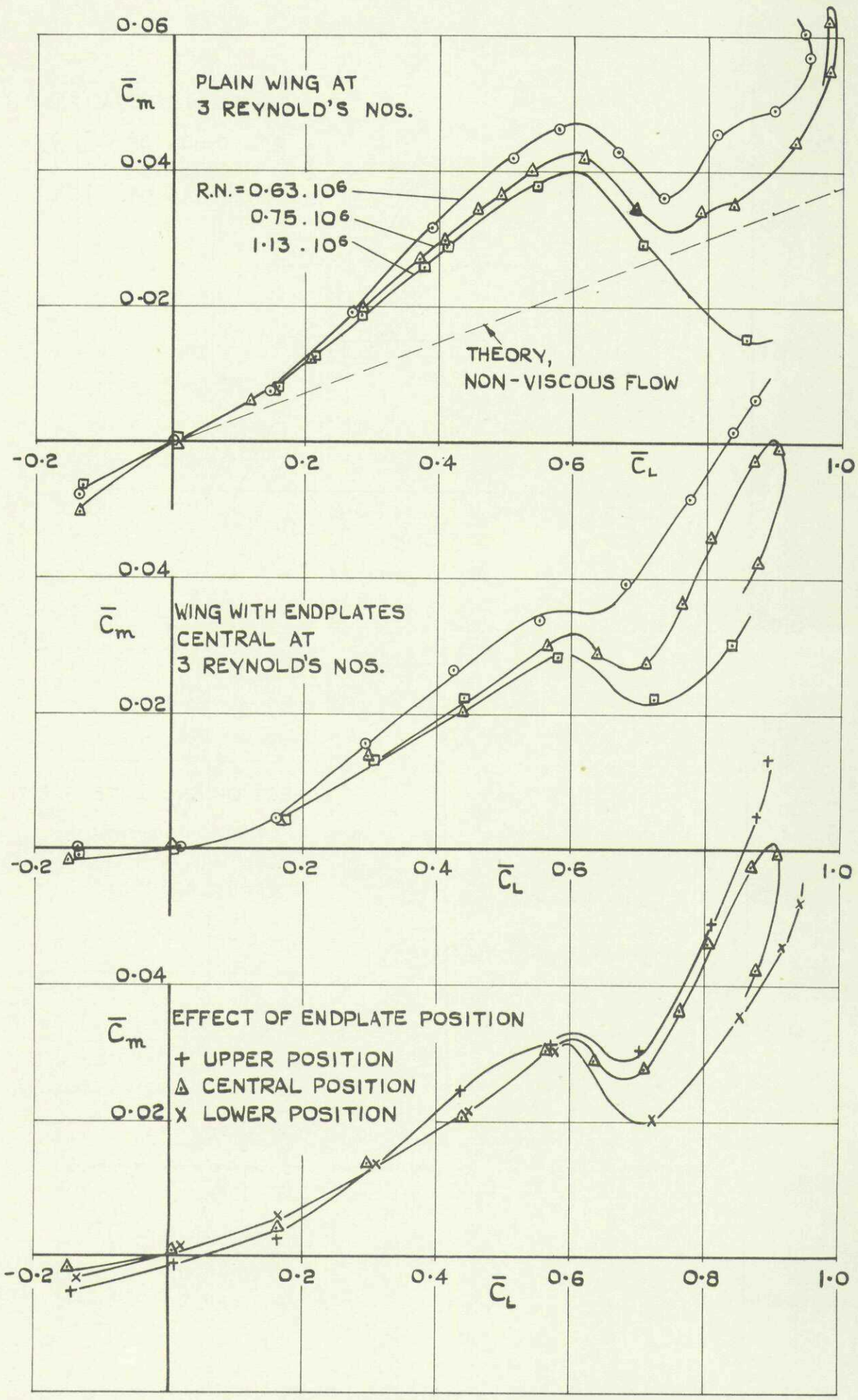


FIG. 7. PITCHING MOMENT COEFFICIENT vs $\bar{C}_L$
EFFECT OF ENDPLATES ON 45° SWEPTBACK WING.
(A.R. = 3·0)

FIG.8.

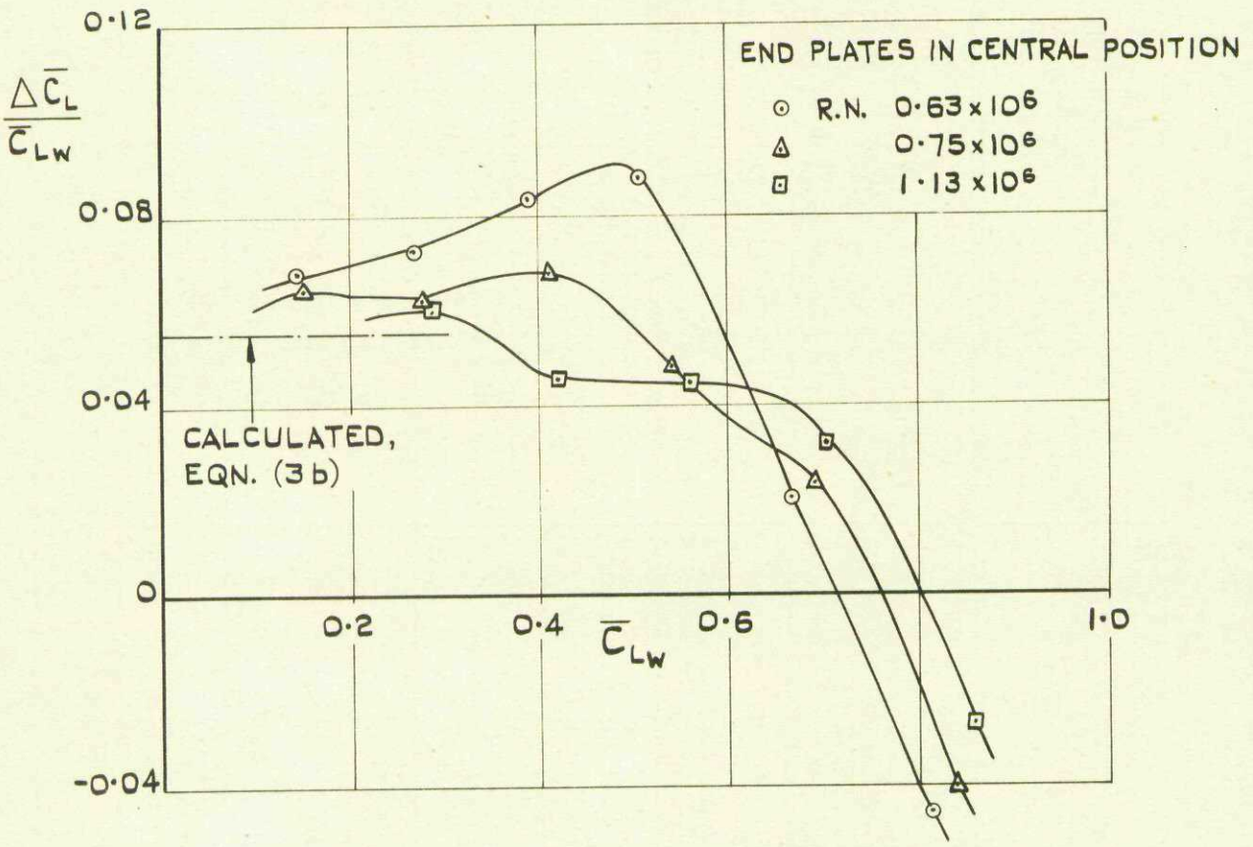


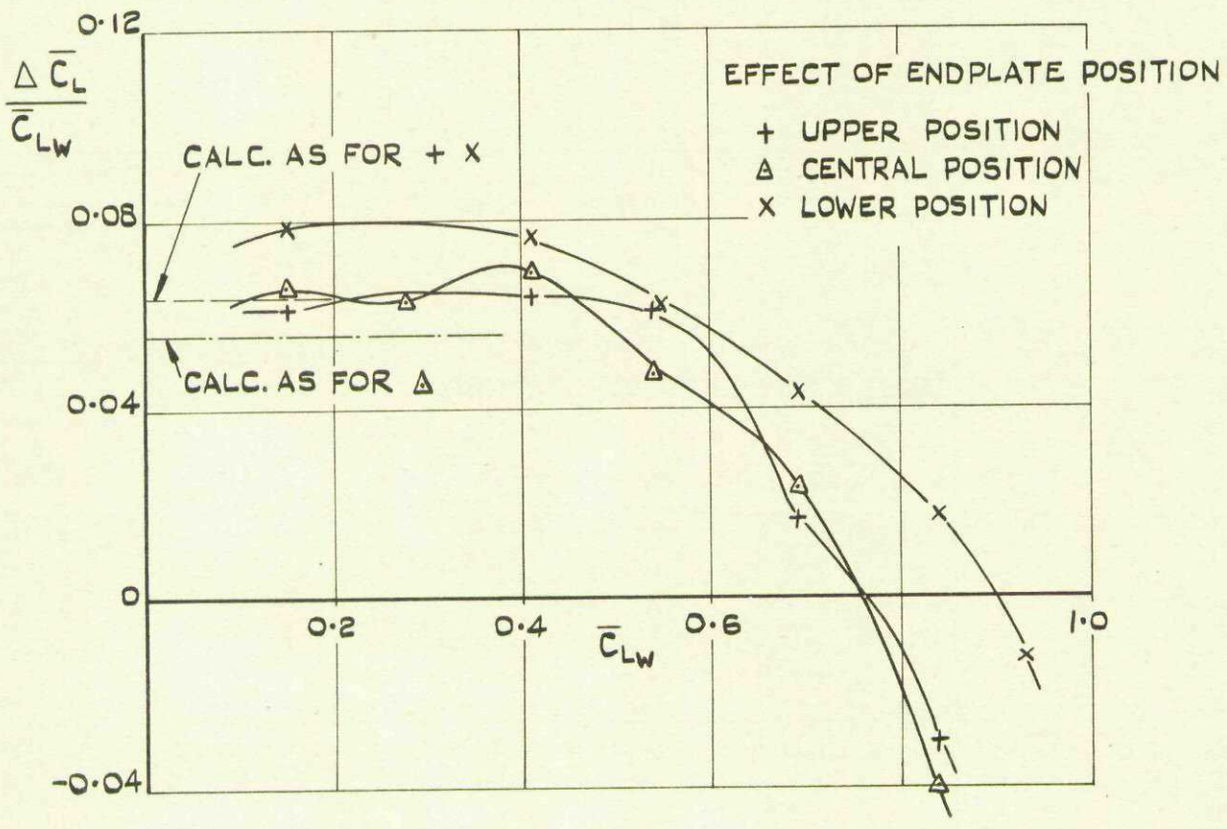


FIG.8. LIFT DIFFERENCES DUE TO ENDPLATES ON 45° SWEPTBACK WING (AS IN FIG. 4.) (A.R.=3·0)

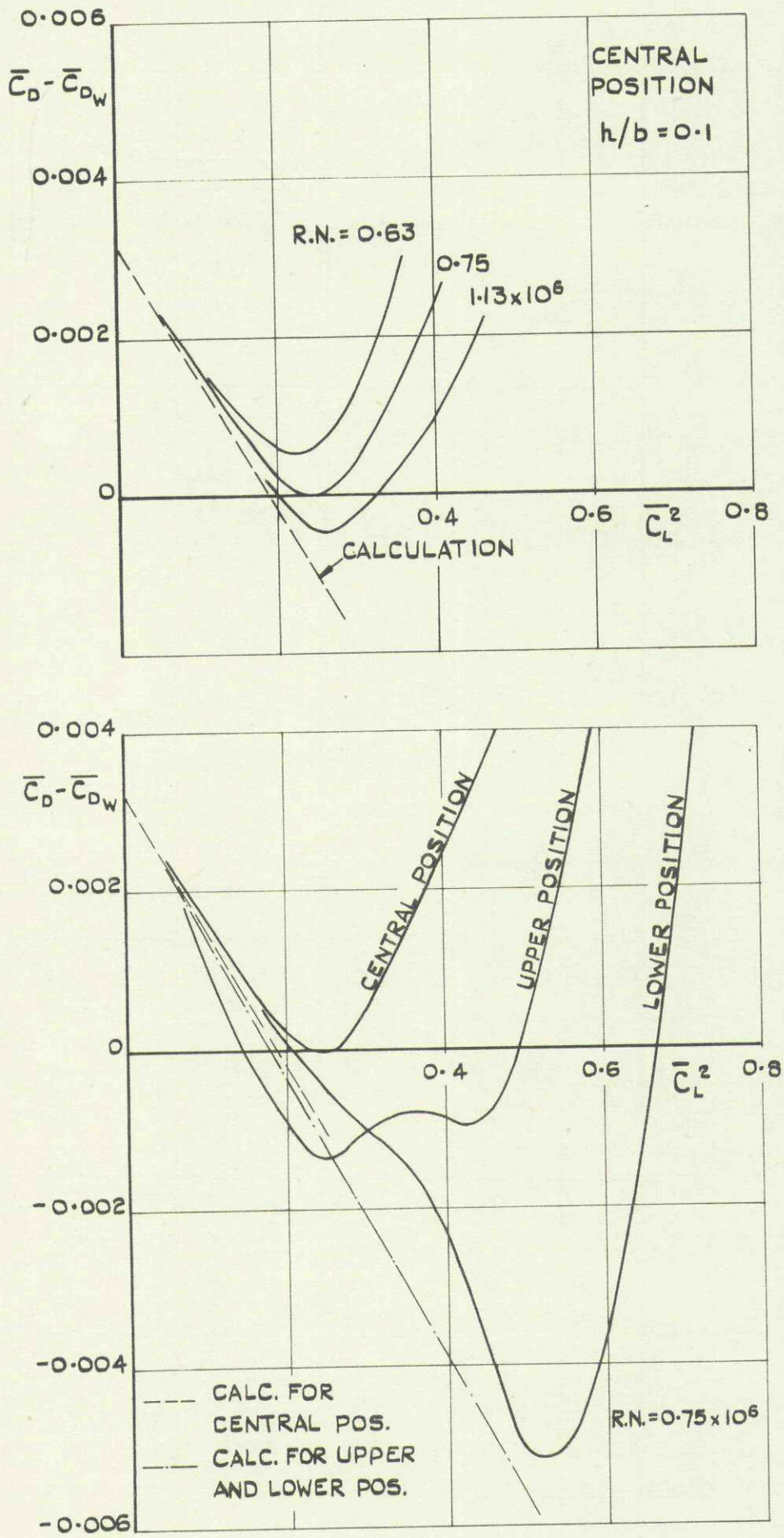


FIG.9. ENDPLATE DRAG vs $\bar{C}_L^2$.
(ENDPLATES AS IN FIG. 4.)

FIG.10.

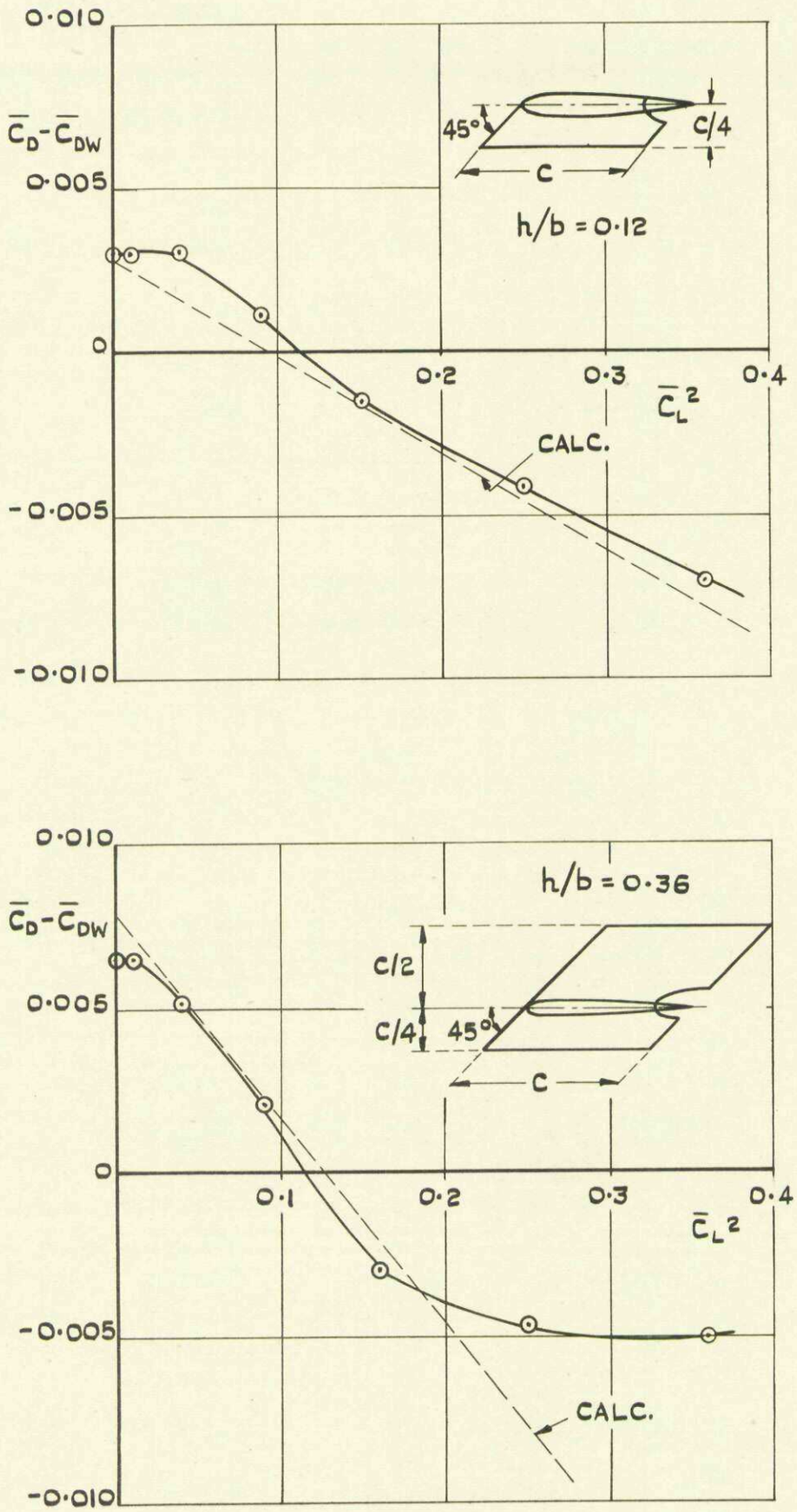


FIG.10. ENDPLATE DRAG. 45° SWEPTBACK WING. ASPECT RATIO 2. CONSTANT CHORD. R.N. = $3.2 \times 10^6$. (FROM REF. 8.)

FIG.11.

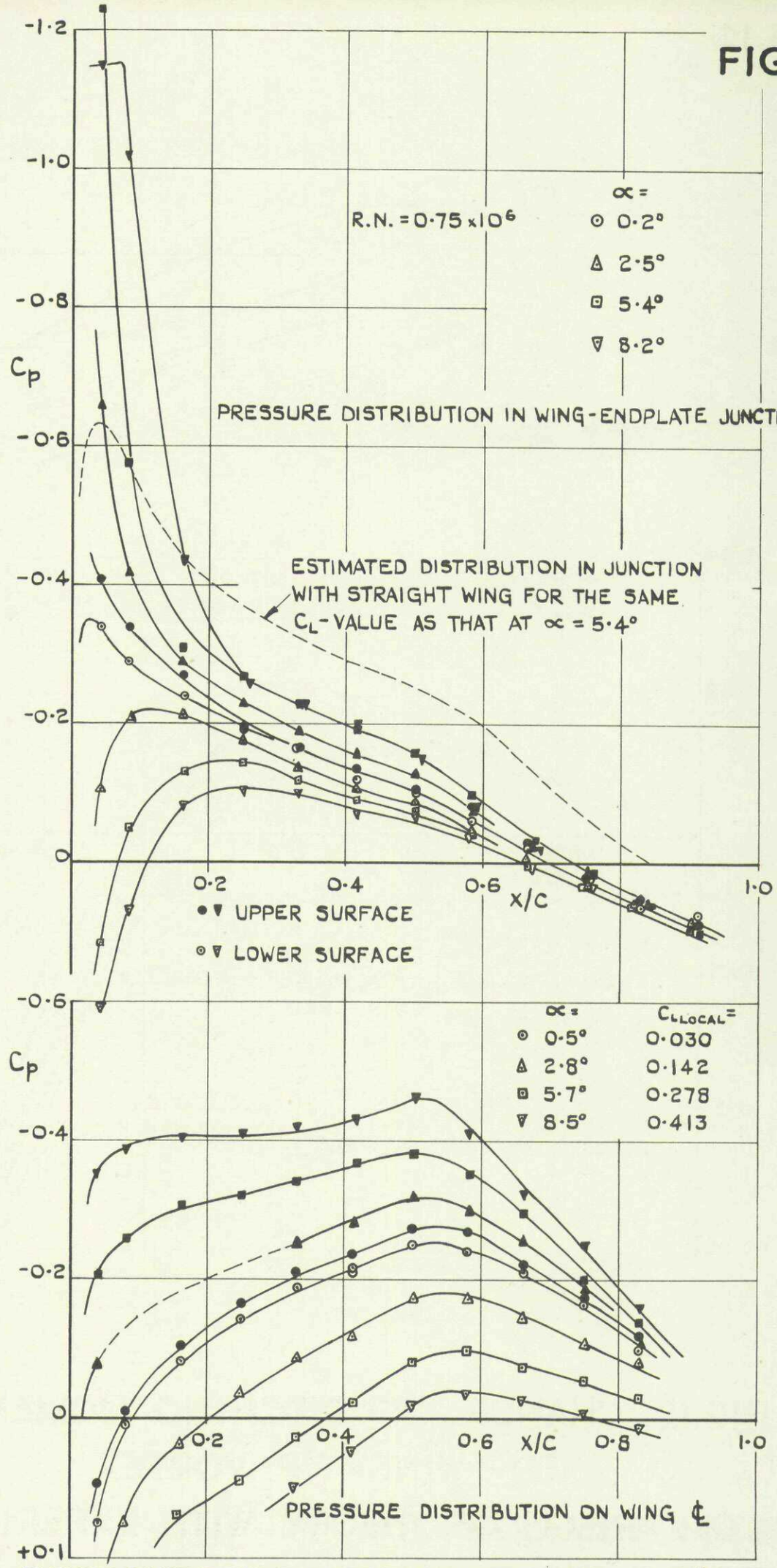


FIG.11. PRESSURE DISTRIBUTION ON 45° SWEPTBACK WING WITH ENDPLATES (A.R. = 3·0)

FIG.12

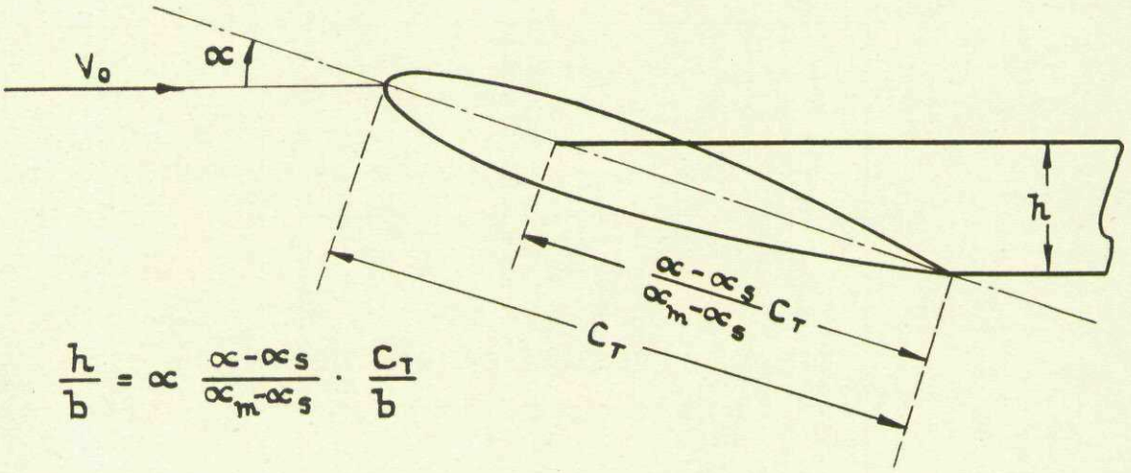


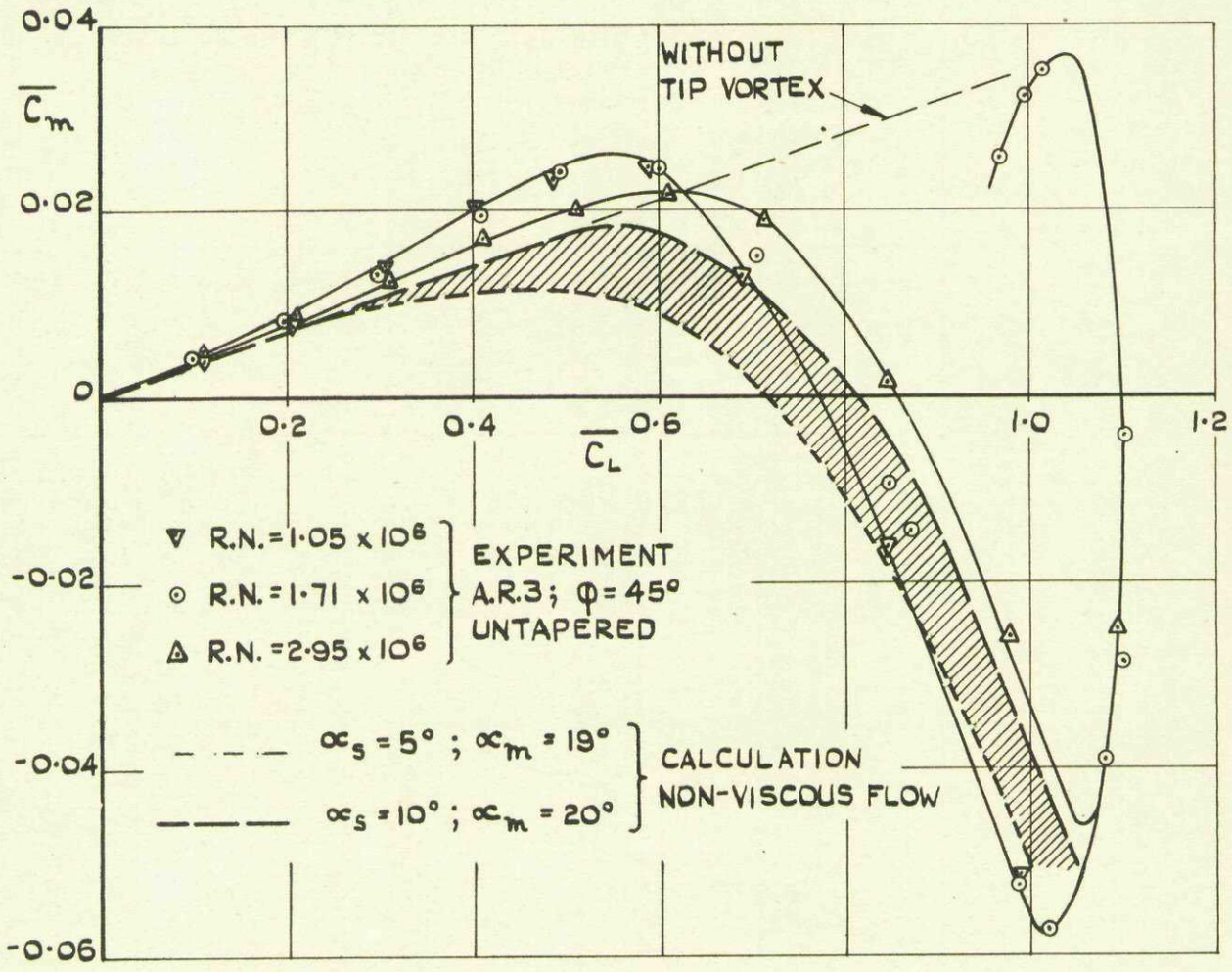


FIG.12. CHANGE OF PITCHING MOMENT DUE TO WING-TIP VORTEX COMPARISON OF THEORY WITH EXPERIMENT.

C.P. No. 104
(14,449)
A.R.C. Technical Report



PUBLISHED BY HER MAJESTY'S STATIONERY OFFICE

To be purchased from

York House, Kingsway, LONDON, W.C.2: 429 Oxford Street, LONDON, W.1
P.O. Box 569, LONDON, S.E.1
13a Castle Street, EDINBURGH, 2 | 1 St. Andrew's Crescent, CARDIFF
39 King Street, MANCHESTER, 2 | Tower Lane, BRISTOL, 1
2 Edmund Street, BIRMINGHAM, 3 | 80 Chichester Street, BELFAST
or from any Bookseller

PRINTED IN GREAT BRITAIN

1952

Price 4s. 0d. net

S.O. Code No. 23-9007-4